A New Method Voltage and Frequency Regulation of Self-Excited Induction Generator Operating in Stand Alone

DHIKRA CHERMITI[1,2] ADEL KHEDHER[1,3]
Renewable Energy and Electric Vehicles (RELEV) (1)
High Institute of Applied Sciences & Technology of Sousse (ISSATS) (2),
Cité Taffala, Ibn Khaldoun, 4003 Sousse-TUNISIA
National Engineering School of Sousse (ENISO) (3),
Route de Ceinture Sahloul, Cité Hammam Maarouf, 4054 Sousse-TUNISIA
dhikra_chermiti@yahoo.fr, adel_kheder@yahoo.fr

Abstract:- This paper proposes a new method to analyze the steady performance of a stand-alone self-excited induction generator (SEIG). The entire system consists on a three-phase induction generator excited with three capacitors-bank and an inductive load. The non linear equations are firstly developed by applying the nodal current approach to the per-phase induction generator, the eventual set of equations is solved using the Newton Raphson algorithm. Simulation results obtained by the proposed method revealed an important effect of several parameters on the self-excitation process. In fact, the load impedance, the prime mover speed and the excitation capacitance value have a direct impact on the terminal voltage and the output frequency of the induction generator. Based on these results, a simple voltage regulation strategy is suggested in order to operate at a fixed power range within tolerable voltage limits.

Key-words:- Induction generator, self-excitation, capacitors-bank, voltage regulation, output frequency.

1 Introduction

These days, the world relies heavily on fossil fuels and nuclear power to generate its electricity. The result is a system that lacks diversity and security, threatens our health, increases the global warming, and robs future generations of clean air, clean water and energy independence. Fortunately, renewable energy resources such as wind, solar, bioenergy and geothermal are capable of meeting a significant proportion of the world's energy needs, and can help to alleviate many of the problems mentioned above while providing other important benefits[1].

A lot of research is being conducted on tapping the advantages of renewable energy such as wind energy which is widely distributed. This kind of energy is often a cheaper option than solar power for rural homes located on distant areas where simplicity and less maintenance are the most wanted features to choose the adequate generator [2]. The induction generator is being increasingly used, in such areas, thanks to its several advantages compared to synchronous generators or DC generators. The induction generator is known by its simplicity, robustness, self protection against overloads and short circuits, reduced unit cost, and capability to operate at variable speed [3-5].

Specially, the later feature promotes the choice of the induction generator to operate in discarded areas where the extension of the grid is usually expensive, difficult and unreliable. When it is connected to the grid, the induction generator can obtain its necessary reactive power from it. Furthermore, the output frequency and the terminal voltage are imposed in the case of the direct connection to the grid [6].However, in a remote area the induction generator is connected directly to the load which brings up the need of an excitation capacitors bank to deliver the required reactive power. Such an excited generator is called Self-Excited Induction Generator (SEIG).

To get an adequate terminal voltage and a suitable frequency to the connected load, the appropriate choice of the excitation capacitance value should be a result of a detailed steady state performances of the SEIG system commonly applied to the per-phase equivalent circuit [7].The loop impedance method or the nodal admittance approaches have usually been the most used methods in many static analyses [8].

Both of them may derive two simultaneous nonlinear equations versus frequency, magnetizing

reactance, capacitor reactance and other SEIG parameters. However different resolution methods are proposed in several published works [9-14].

A numerical method using routine "fsolve" MATLAB function was proposed by [9] to formulate the problem of a SEIG with a torque-speed characteristic of the prime mover. In [10], the authors investigated a direct algorithm to minimize the induction generator's admittance without decoupling its real and imaginary parts in order to analyze the SEIG performances. In [11], the authors proposed some different ways based on the eigenvalue method determination for minimum and maximum values of capacitance required to self-excite an isolated single phase induction generator.

In [12], a mathematical model of a SEIG connected to a bridge rectifier was derived and proved that the three-phase SEIG can operate under static power conversion loads.

In [13], an automatic mode switch method based on a phase-locked loop controller was presented. This method uses a flexible digital signal processor (DSP) system that allows the user-friendly code development and online tuning to be used to implement and test the different control strategies.

Different static approaches previously mentioned are the basis of most SEIG control strategies. Yet, most of them are settled for a simply resistive load in addition of the poor voltage regulation that remains the inherent drawback for such methods[14].

In distant areas, a slight variation on voltage or on frequency is commonly tolerable by loads connected in such a stand.

Hence, the use of sophisticated and high cost converters to regulate the terminal voltage or output frequency cannot be justifiable. Indeed, simple regulators, and reliable and low-cost control strategies are required in discarded areas where the maintenance requirements are minimized.

This work proposes a simple method of voltage and frequency control to maintain the terminal voltage within acceptable limits of an induction generator operated in stand alone, using the Newton Raphson method.

The paper is organized as follows: A second section illustrates the Newton-Raphson algorithm applied to the per phase simplified equivalent circuit of the SEIG. Also, a set of nonlinear equations derived from the loop current approach is developed. The application of this method to a 7.5kW induction generator and the simulation results of the steady SEIG performances are described in section three.

We highlight the importance of the constant terminal voltage operation of the SEIG in the fourth section. The stator voltage control strategy and excitation capacitors computing required to maintain a given stator voltage are detailed in section five. The paper ends up with a general conclusion.

2 Newton-Raphson algorithm applied to the stand alone SEIG system

The steady analysis of the SEIG is based on the per-phase equivalent circuit of the induction generator shown in Fig.1. This circuit is normalized to the Raphson algorithm applied to the per-phase simplified equivalent circuit of the SEIG. Also, a set base frequency by dividing all the parameters by the per unit F .

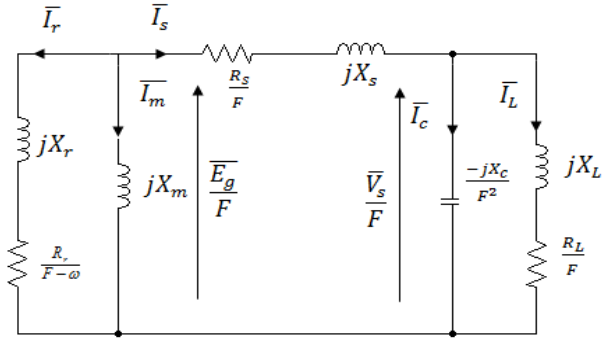

Fig. 1. Per-phase equivalent SEIG circuit

In this study, we neglect the iron losses [11] and all machine parameters are assumed constant, except the magnetizing reactance which varies against the air gap voltage of the SEIG [15]. In the literature, there are several ways to represent the relationship between E_g and X_m [16-21].

In our case, the magnetizing curve is approximated by the polynomial equation where the coefficients are determined using the fitting MATLAB technique function and illustrated by Fig.2.

$$\frac{E_g}{F}(X_m) = k_3 X_m^{\,3} + k_2 X_m^{\,2} + k_1 X_m + k_0 \qquad (1)$$

k_3, k_2, k_1 and k_0 are given in appendix A.

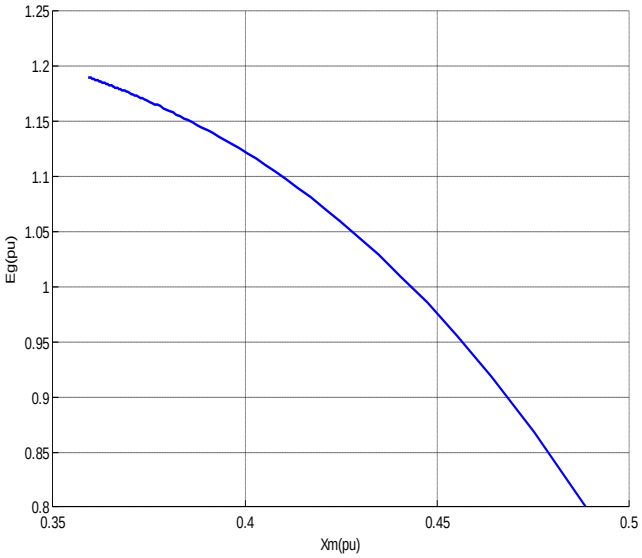

Fig. 2. Magnetizing curve of 7.5 kW- 220 V induction generator

In order to simplify the previous model, we can reduce all circuit impedances on three serial impedances $\overline{Z}_1$, $\overline{Z}_2$ and $\overline{Z}_3$. Therefore, the simplified per-phase circuit becomes as follows :

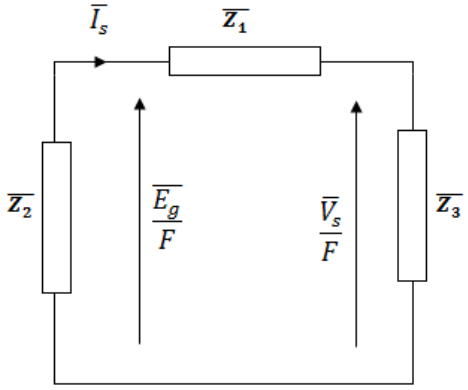

Fig. 3. Simplified per-unit SEIG per phase circuit

Where:

$$\overline{Z}_1 = \frac{R_S}{F} + jX_S \tag{2}$$

$$\overline{Z}_2 = \frac{\left(jX_m\right)\left(\frac{R_r}{F-\omega} + jX_r\right)}{\left(jX_m\right)+\left(\frac{R_r}{F-\omega} + jX_r\right)} \tag{3}$$

$$\overline{Z}_3 = \frac{\left(-\frac{jX_C}{F^2}\right)\left(\frac{R_L}{F} + jX_L\right)}{\left(-\frac{jX_C}{F^2}\right)+\left(\frac{R_L}{F} + jX_L\right)} \tag{4}$$

Let us consider the first Kirchhoff 's law to the circuit given by Fig. 2, so we can write:

$$\overline{I}_S\,\overline{Z}_T = 0 \tag{5}$$

with $\overline{Z}_T = \overline{Z}_1 + \overline{Z}_2 + \overline{Z}_3$

Since at a normal operation mode, the stator current is different to zero, then we obtain:

$$\overline{Z}_T = 0 \tag{6}$$

After some demonstrations, the real and imaginary parts of $\overline{Z}_T$ are arranged on two polynomial, such as:

$$\begin{cases} f_1 = \mathrm{Im}\left(\overline{Z}_T\right) = 0 \\ f_2 = \mathrm{Re}\left(\overline{Z}_T\right) = 0 \end{cases} \tag{7}$$

where the functions expressions are given by :

$$f_1 = a_7F^7 + a_6F^6 + a_5F^5 + a_4F^4 + a_3F^3 + a_2F^2 + a_1F$$

$$f_2 = b_6F^6 + b_5F^5 + b_4F^4 + b_3F^3 + b_2F^2 + b_1F + b_0$$

with:

$$a_1 = \varepsilon_6X_C^2 - \alpha_6R_L^2$$

$$a_2 = -2v\varepsilon_3X_C^2 + R_L^2\alpha_2X_C$$

$$a_3 = \varepsilon_3X_C^2 - \varepsilon_4X_C + \varepsilon_5$$

$$a_4 = 2v\left(-\varepsilon_1X_C - R_L^2\alpha_1\right)$$

$$a_5 = \varepsilon_1X_C + \varepsilon_2 \quad , \quad a_6 = -2X_L^2v.\alpha_1$$

$$b_0 = \beta_6\alpha_6X_C^2 \quad , \quad b_1 = -v\delta_1X_C^2$$

$$b_2 = \left(R_L\alpha_2 + \delta_2\right)X_C^2 + \left(2X_L\delta_3\right)X_C + \beta_5\alpha_6$$

$$b_3 = \left(2X_Lv\delta_4\right)X_C - R_L^2v\delta_4$$

$$b_4 = -2\delta_5X_C + \left(\delta_6X_L^2 + \beta_4X_m + \beta_5\alpha_2\right)$$

$$b_5 = -X_L^2v\delta_4 \quad , \quad b_6 = X_L^2\delta_2$$

All coefficients α_i , ε_i , β_i and δ_i for $\left(i = 1...6\right)$ are given in appendix B.

These two previous equations can be solved simultaneously for any two unknown ones. When the required capacitance to self-excite the induction generator is known, X_m and F are chosen as variables. In another case, for a given magnetizing reactance X_m of the SEIG, we can determine X_C and F . Thus, we can write:

$$f\left(X\right) = 0 \tag{8}$$

where $f = \left[f_1 \quad f_2\right]^T$

And $X = \left[X_m \quad F\right]^T$ or $X = \left[X_C \quad F\right]^T$

The set of equations (7) is then solved by the Newton-Raphson algorithm which is one of the fastest and quadratic convergences to the solution.

Referring to Fig.1, the stator current $\overline{I}_S$, rotor current $\overline{I}_r$, load current $\overline{I}_L$ and the capacitance

current $\bar{I}_C$ are expressed, respectively, by following equations.

$$\bar{I}_S = \frac{\frac{\bar{E}_g}{F}}{\bar{Z}_1 + \bar{Z}_3} \quad (9)$$

$$\bar{I}_r = \frac{\frac{\bar{E}_g}{F}}{\frac{R_r}{F-v} + jX_r} \quad (10)$$

$$\bar{I}_L = \frac{\bar{V}_S}{R_L + jFX_L} \quad (11)$$

$$\bar{I}_C = \frac{\bar{V}_S}{\frac{-jX_C}{F}} \quad (12)$$

The active power P_L and the reactive power Q_L absorbed by the load are :

$$\begin{cases} P_L = 3\left|\bar{I}_L\right|^2 R_L \\ Q_L = 3\left|\bar{I}_L\right|^2 FX_L \end{cases} \quad (13)$$

3 Simulation results

The proposed system consists in a four poles, 10HP three-phase induction generator connected to a variable (RL) load. The nominal voltage generator and the rotor speed are respectively 220V and 1500rpm.

The SEIG steady state performance depends essentially, on the rotor speed, the excitation capacitor and the load impedance.

3.1 Minimum excitation capacitor computing

As a first step of the SEIG steady state analysis, we have to compute the minimum excitation capacitor value that can ensure a successful excitation process. Thus, the resolution of equation (7) reveals the excitation capacitors values that coordinate with the load impedance variations. Fig. 5 shows the required excitation capacitor versus load power for different inductance load values and Fig.6 generalizes these variations versus the power factor from 0.7 to 1.

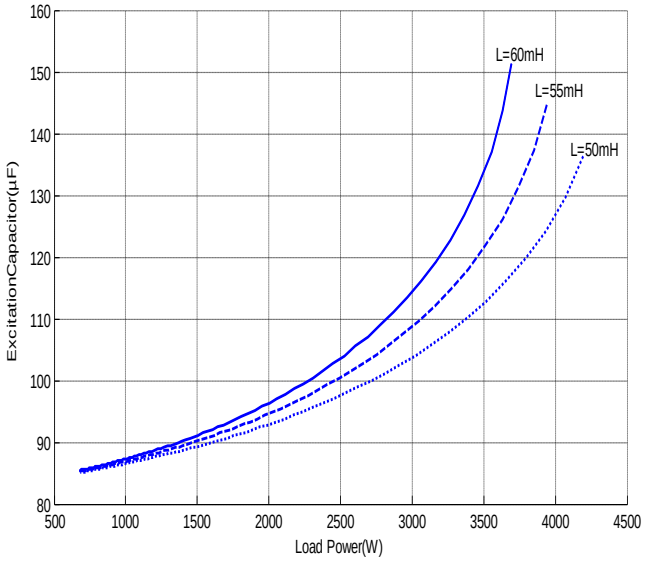

Fig. 4. Excitation capacitance versus load power for different inductance loads

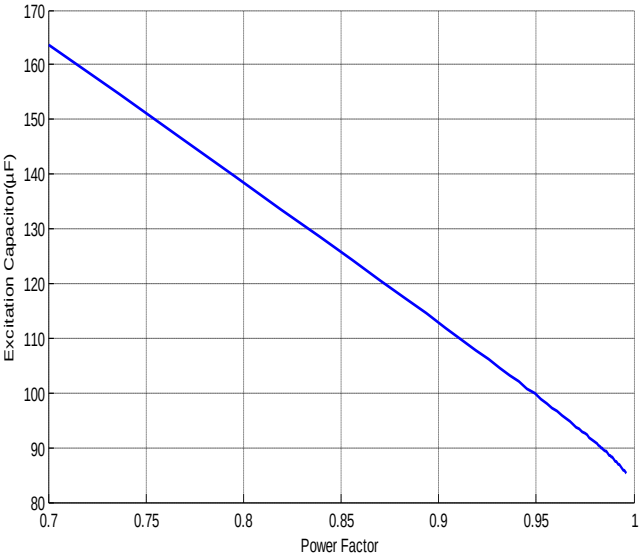

Fig. 5. Excitation capacitance versus power factor

One can observe that the excitation capacitance value rises when the required reactive power increases. This is due to the fact that the computed capacitance has to deliver the reactive supplies of both the magnetizing inductance of the SEIG and the inductance load.

The capacitance excitation variation is fitted to the following quadratic equation:

$$C_{ex\,\min} = -113.6 p_f{}^2 - 66.867 p_f + 256.26 \quad (14)$$

Thus, for a predetermined load value we can compute the appropriate excitation capacitor. However, a loaded SEIG operating with a specific capacitance can lose its self-excitation if the speed is increased above or decreased below given values.

3.2 Effect of Rotor speed and load impedance

Wind speed is the most random parameter in our system. Any variation in wind speed affects the rotor speed of the induction generator which influences, in turn, the generated voltage and also the output frequency. To emphasize this effect on the steady SEIG performances, we have chosen the excitation capacitance at 125µF, according to the computed values mentioned in the previous section, then we have varied the load impedance gradually for some values of the rotor speed (ω=0.9pu, 1pu and 1.1pu). Fig.6 and Fig.7 show the variation of the terminal voltage, respectively, versus the load power and the power factor for different rotor speed values.

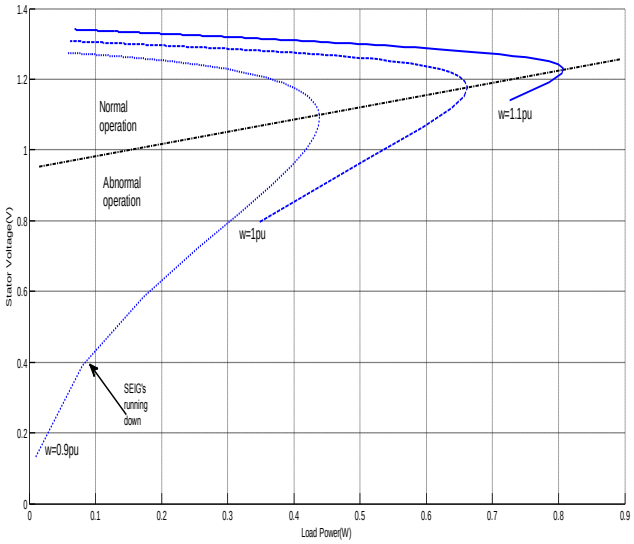

Fig. 6. Output voltage versus load power for different rotor speeds

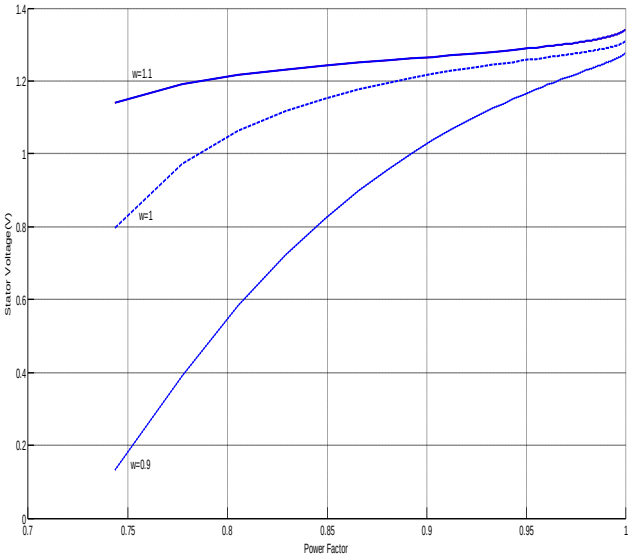

Fig. 7. Terminal voltage versus load power factor for different rotor speeds

Fig.8 illustrates the terminal voltage versus load power for some inductance values and the output frequency versus the load power at different rotor speed values is shown by Fig.9.

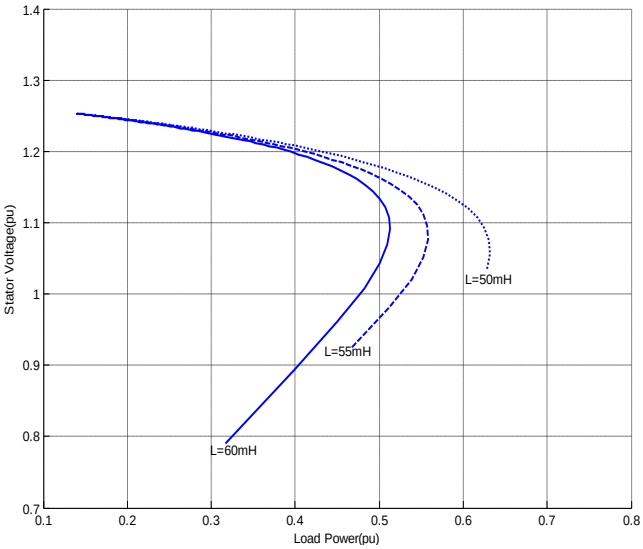

Fig. 8. Stator voltage against load power for different inductance loads

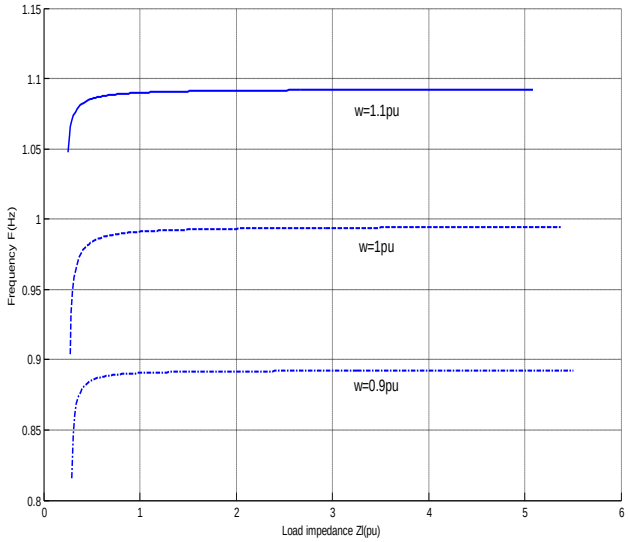

Fig. 9. Output frequency versus load power for different rotor speeds

A reduction in the load impedance implies a decrease in the terminal voltage and the SEIG system operates normally until it reaches the maximum load power point where the induction generator risks to stall untimely, chiefly if it is accompanied by a speed diminution as it seems in Fig.6 when the rotor speed is equal to 0.9pu. However, the increase in the prime mover speed has extended this maximum power point from 0.43pu to 0.8pu which restricts the abnormal operation zone. Thus, to compensate this fall stator voltage we ought to increase the prime mover speed. As a result, the SEIG generates a higher load power and delay the generator stall; yet, it can cause a large

output frequency variation and the stator voltage exceeds its nominal value.

The voltage large drop seen in Fig.7, especially when feeding an important inductive load, represents the main disadvantage of the SEIG and can be referred to the under excitation of the machine[21]. In fact, the decrease of the power factor is the origin of the rise of the reactive power requirements which demands an increasing of the required excitation capacitance to recover the reactive power lack. This weak excitation can be also observed from Fig.8 where the terminal voltage is greatly sensitive to any slight variation of the inductance load.

The output frequency is also affected by the load impedance value. Indeed the increase in the load power is automatically attached to a sliding rise which leads to a frequency decrease; such behavior can be noted in Fig.9.

3.3 Effect of excitation capacitance value

When the SEIG is operating at a fixed rotor speed and if the connected load is variable, switching on different capacitance values is recommended to supply the necessary reactive power to the whole system and then ensuring the self excitation process. The resolution of equation (7) for different excitation capacitances calculated by the Newton-Raphson algorithm has led to the following terminal voltage variations versus the load power.

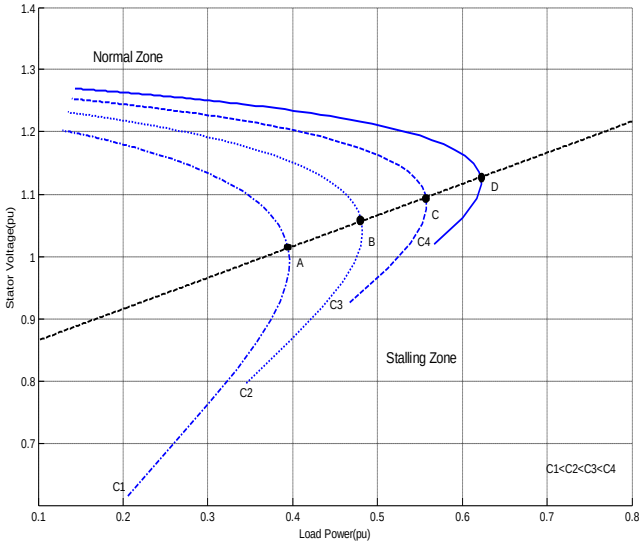

Fig. 10. Output voltage versus load power for different capacitances at v=1pu

According to Fig.10, we note that the terminal voltage follows a parabolic shape for each value of the excitation capacitor. While the SEIG is progressively loaded, the terminal voltage decreases smoothly which is due to the positive sign of the load power derivative versus stator voltage. This operation part is called "normal operation zone". This variation continues until the derivative sign becomes negative and the maximum power is reached: such behavior is named "stalling zone" where the SEIG risks to fail to self excite. However, it has proven that raising the self-excitation capacitance has increased both the maximum output power of the SEIG $P_{L\max}$ and the dropped stator voltage V_{Sdrop} has enhanced from point A to point D, as given in Fig.10.

Hence, depending on the connected load, each of those capacitors have allowed operating at a fixed range of load power.

The important influence of these parameters, previously mentioned, on the output frequency and the terminal voltage of the SEIG which reveals the necessity of voltage and frequency regulation.

4 Stator voltage optimization

Since the SEIG has successfully built up its voltage, the next interest difficulty is to maintain the terminal voltage at a predetermined value as the load increases. Using the same proposed algorithm for computing capacitance, an additional equation is also developed for calculating the capacitance requirements of the loaded SEIG in order to obtain a constant terminal voltage.

According to Fig.2, the stator voltage can be written as:

$$\overline{V}_S = \frac{\overline{Z}_3}{\overline{Z}_3 + \overline{Z}_1}\overline{E}_g \tag{15}$$

Consider that the stator voltage is to be maintained within $\pm 5\%$ of its nominal value 220V. For reasons of simplicity, we have begun by keeping constant no load stator voltage. To do, a third equation is needed to be inserted to equation (7) which its expression is:

$$f_3 = \left|\frac{\overline{Z}_3}{\overline{Z}_3 + \overline{Z}_1}\right| \overline{E}_g - \overline{V}_{\lim} = 0 \tag{16}$$

For a given load, the stator voltage depends on the capacitor reactance X_C and on the air-gap voltage ($E_g = f(X_m)$). So, the system of equations becomes:

$$\begin{cases} f = [f_1 \quad f_2 \quad f_3]^T = 0 \\ X = [X_m \quad F \quad X_C]^T \end{cases} \tag{17}$$

The variation of excitation capacitors against the rotor speed at the maintained constant stator voltage

value is illustrated below. The maximum and the minimum limit voltage V_{max} and V_{min} are also represented by dotted curves.

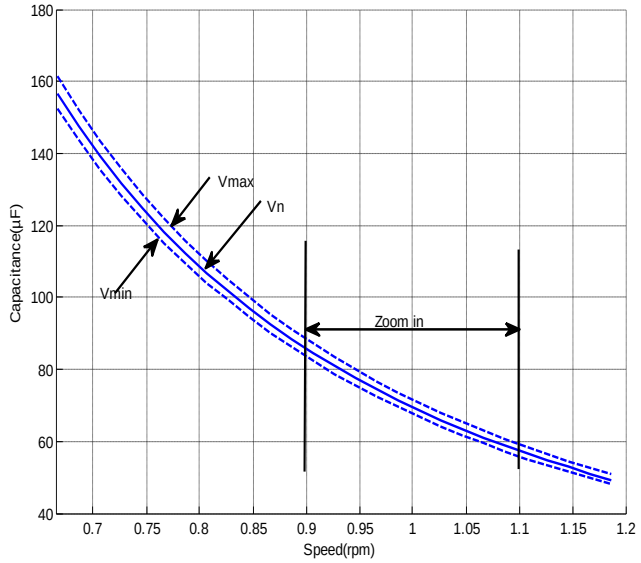

Fig. 11. Variation of excitation capacitors versus rotor speed to maintain constant voltage

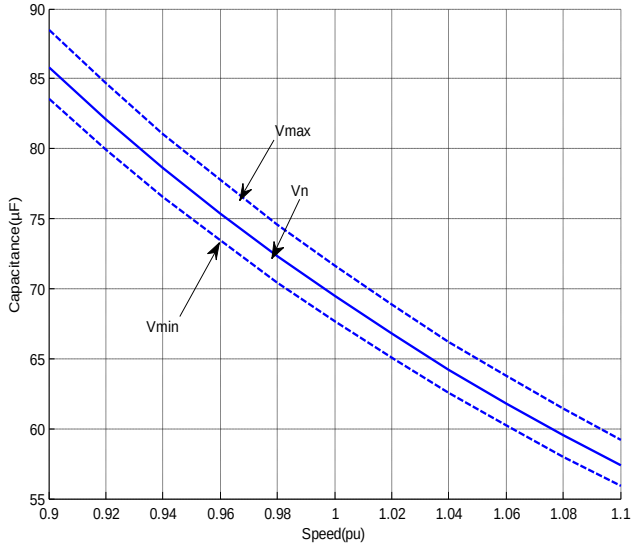

Fig. 12. Zoom in of excitation capacitors against rotor speed between 0.9 and 1.1pu

Fig.11 indicates that the required excitation capacitance is inversely proportional to the prime mover speed. Therefore, to keep an eligible terminal voltage, we should either increase the value of the rotor speed or the value of the excitation capacitance. Fig.12 illustrates the Zoom of the same curves given in Fig.11.

5 Stator voltage regulation

In previous sections, it has been noticed that the evident drawback of the SEIG system was its poor voltage regulation [23]. Providing that the rotor driving speed is kept constant, a single adjustment of the capacitance excitation value should maintain the terminal voltage constant. To achieve this purpose, we have determined the appropriate capacitance value to ensure that the system operates within the stator voltage limits.

Considering that the terminal voltage of the induction generator is to be maintained within ±5% of its rated value, the set of equations (17) is then solved for the constant terminal voltage V_{max} and V_{min} and the corresponding capacitor-load power characteristics are represented by a solid line and a dotted one, respectively, in Fig.13. We calculate C_0 as the capacitance that can deliver a maximum voltage for the no-loaded SEIG. We have assumed that the SEIG is driven by a regulated turbine at the synchronous speed, so we have fixed the per unit speed at 1pu and we have loaded progressively the SEIG by an inductive load.

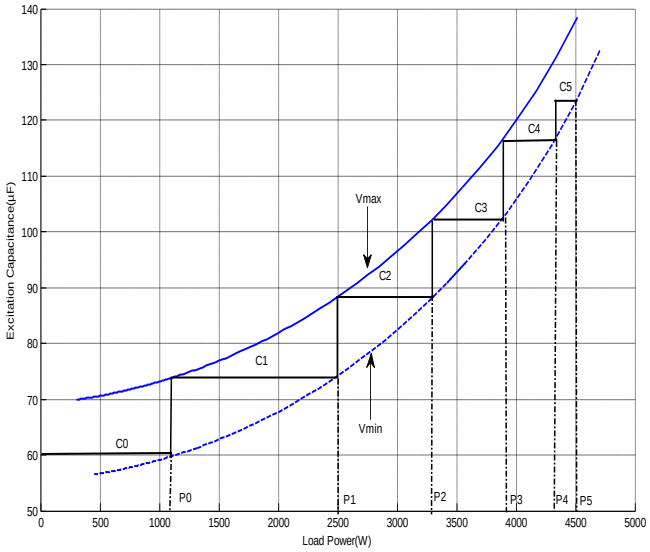

Fig. 13. Variation of excitation capacitance against output power for constant terminal voltage within ±5%

Each value of the excitation capacitance allows the SEIG to operate at a fixed range of power with a ±5% voltage tolerance. To switch between two ranges, we have to insert an additional capacitance calculated as:

$$C_{addj} = C_j - C_{j-1} \text{ ; where } j = 1,2...5 \quad (18)$$

All computed values are detailed in the following table.

Table3. Capacitance values to keep terminal voltage within ±5%

	[0-P_0]	**[P_0-P_1]**	**[P_1-P_2]**	**[P_2-P_3]**	**[P_3-P_4]**	**[P_4-P_5]**
Power range (W)	0-1106	1106-2501	2501-3294	3294-3892	3892-4330	4330-4500
C_{exT} (µF)	60.5	74.25	88.16	102.7	116.6	123.3
C_{addj} (µF)	0	C_{add1}= 13.75	C_{add2}= 13.91	C_{add}=14.54	C_{add4}=13.9	C_{add5}=6.7

Based on these results, we can regulate the terminal voltage between two tolerable limits by a simple switching of the capacitance values. It may be noted that the number of steps augments as well as the auxiliary capacitors branches, when the voltage tolerance becomes tighter (i.e. ±3%, ±2%).
Such results can be investigated to connect the appropriate excitation capacitance according to the required load as it is illustrated by Fig.14.

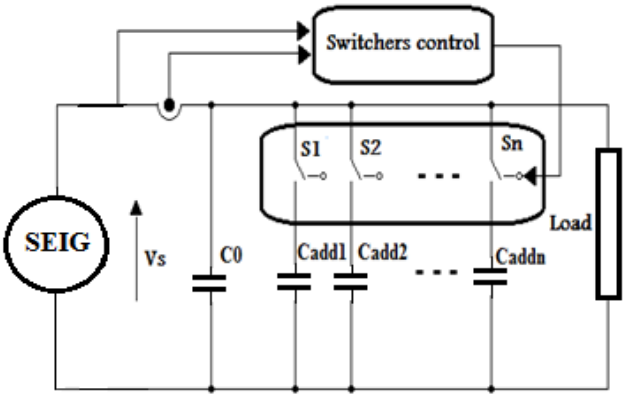

Fig .14. Per phase circuit of the terminal voltage regulation process

We note that switchers $S_1, S_2, ...S_n$ in Fig.14 may be thyristors or electrical relays which allow

inserting or not an auxiliary capacitor to keep the terminal voltage in its admissible value despite the load power variations.

6 Conclusion:

An adequate method of terminal voltage control of a SEIG operating in stand alone is illustrated in this paper. This method consists in keeping the stator voltage between upper and lower defined limits by the evaluation of the necessary values of the excitation capacitors.
This has required a detailed steady state analysis of the SEIG using the equivalent per-phase circuit. A set of equations of the loaded SEIG have been developed and solved using the Newton-Raphson algorithm. The resolution results are investigated to demonstrate different relationships between the loaded SEIG outputs and its different parameters.
Rotor speed has a minimum value for which self-excitation process can occur without the stall down of the SEIG also an excessive rise on it can affect directly the frequency accuracy of the whole system. The adequate selection of the computed excitation capacitors have supplied the necessary reactive power to the SEIG system in order to enlarge the normal operation zone and to raise the maximum dropped stator voltage especially when the power factor load is decreasing.
For self-excitation process it is not only the values of capacitor and rotor speed that matters but also if the SEIG reaches its maximum magnetizing reactance X_m which makes the loss of remanent magnetic flux from the core so possible, Then there will be no self-excitation. Once the remanent magnetic flux is lost the SEIG ought to be run as a motor or the capacitors should be charged to allow the SEIG to self-excite again.

Nomenclature

R_S	stator resistance
R_r	rotor resistance
X_S	stator leakage reactance
X_r	rotor leakage reactance
X_m	magnetizing reactance
X_C	capacitor reactance
R_L	load resistance
X_L	load reactance
F	per unit frequency (pu)
ω	per unit rotor speed
$\overline{V}_S$	stator voltage
$\overline{E}_g$	air gap voltage
$\overline{I}_S$	stator current

$\bar{I}_r$ rotor current
$\bar{I}_L$ load current
$\bar{I}_C$ capacitance current
$C_{ex\min}$ minimum excitation capacitor
C_{exT} total excitation capacitor
$P_{L\max}$ maximum load power
V_{Sdrop} maximum dropped voltage
C_{add} additional capacitor value

Appendix A.

Induction generator parameters

Nominal rated power	P_n=7500W
Nominal rated voltag**e**	V_{sn}=220V
Nominal frequency	f =50Hz
Pairs pole number	p =2
Stator resistance	R_s =0.7384Ω
Rotor resistance	R_r =0.7402Ω
Stator leakage reactance	X_s =0.9561H
Rotor leakage reactance	X_r =0.9561H
Base voltage	V_b=220V
Base frequency	F_b=50Hz
Base rotor speed	N_b=1500rpm
Base impedance	Z_b=100 Ω

Appendix B.

- The coefficients of the magnetizing curve in per unit system are:

$k_3 = -34$, $k_2 = 27$, $k_1 = -7.6$ and $k_0 = 2$.

- Equation(7) Coefficients expressions

$$\alpha_1 = \left(X_m + X_r\right)\left(X_m X_r + X_m X_S + X_r X_S\right)$$
$$\alpha_2 = \left(X_m + X_r\right)^2, \alpha_3 = R_r^2\left(1 + X_S\right)$$
$$\alpha_4 = R_r^2\left(X_m + X_S\right), \alpha_5 = R_r^2\left(X_m + X_r\right)$$
$$\alpha_6 = \left(R_r^2 + v^2\alpha_2\right)$$
$$\varepsilon_1 = \left(-\alpha_2 X_L^2 - 2\alpha_1 X_L\right)$$
$$\varepsilon_2 = \left(v^2\alpha_1 + \alpha_3\right)X_L^2 + R_L^2\alpha_1$$
$$\varepsilon_3 = \left(\alpha_2 X_L + \alpha_1\right)$$
$$\varepsilon_4 = \left[\alpha_6 X_L^2 + \left(2v^2\alpha_1 + \alpha_4\right)X_L + R_L^2\alpha_2\right]$$
$$\varepsilon_5 = R_L^2\left(\alpha_4 + \alpha_1\right)$$
$$\varepsilon_6 = \left(\alpha_6 X_L + \alpha_5 + v^2\alpha_1\right)$$

And

$$\beta_1 = R_r X_m^2, \beta_2 = R_S\alpha_2, \beta_3 = R_r^2 R_S, \beta_4 = R_L^2 R$$
$$\beta_5 = R_L^2 R_S, \ \beta_6 = \left(R_L + R_S\right)$$
$$\delta_1 = \left(2\alpha_2\beta_6 + \beta_1\right), \delta_2 = \left(\beta_1 + \beta_2\right)$$
$$\delta_3 = \left(\beta_2 + \beta_3\right), \delta_4 = \left(\beta_1 + 2\beta_2\right)$$
$$\delta_5 = \left(\beta_1 + \beta_2 X_L\right), \delta_6 = \left(\beta_3 + v^2\beta_2\right)$$

References:

[1] A. M. Kassem, Robust voltage control of a stand alone: wind energy conversion system based on functional model predictive approach. *Electrical Power and Energy Systems*,Vol 41, 2012, pp. 124–132.

[2] J. Alaya, A.Khedher and M.F. Mimouni, DTC and Nonlinear Vector Control Strategies Applied to the DFIG operated at Variable Speed, *WSEAS Transactions on environment and development*, vol. 6, No. 11, November 2010, pp. 744-753.

[3] N. Khmiri, A.Khedher and M.F. Mimouni, An Adaptative Nonlinear Backstepping of DFIG Driven by Wind Turbine, *WSEAS Transactions on environment and development*, vol. 8, No. 2, April 2012, pp. 744-753.

[4] B. Singh, S. P. Singh, M. Singh, R. Dixit, N. Mittal and A. Barnwal, Stand alone power generation by asynchronous generator: a comprehensive survey 3φ. *International Journal of Reviews in Computing*, Vol. 10, July 2012.

[5] R.C. Bansal, Three-phase self-excited induction generators: An overview. *IEEE Trans. on Energy Conversion*, Vol. 20, No. 2, 2005, pp.292-299.

[6] S.A. Deraz, F.E. Abdel Kader, A new control strategy for a stand-alone self-excited induction generator driven by a variable speed wind turbine. *Renewable Energy*, Vol. 51, 2013, pp.263-273.

[7] T. Ahmed, K. Nishida and M. Nakaoka, A novel stand-alone induction generator system for AC and DC power applications. *IAS, IEEE*, 2005, pp. 2950-2957.

[8] G. V. Jayaramaiah and B. G. Fernandes, Novel voltage controller for stand-alone induction

generator using PWM-VSI. *IEEE,* 2006, pp. 204-208.

[9] M. H. Haque, Characteristics of a stand-alone induction generator in small hydroelectric plants. *Australasian Universities Power Engineering Conference AUPEC'08*, December 2008, Sydney, pp. 42-47.

[10] A. Kheldoun, L. Refoufi, D. E. Khodja, Analysis of the self-excited induction generator steady state performance using a new efficient algorithm Electric. *Power Systems Research*, Vol. 86, 2012, pp. 61– 67.

[11] S.N. Mahato , S.P. Singh, M.P. Sharma, Excitation capacitance required for self excited single phase induction generator using three phase machine. *Energy Conversion and Management*, Vol. 49, 2008, pp.1126–1133.

[12] A.I. Alolah, Static power conversion from three-phase self-excited induction and reluctance generators. *Electric Power Systems Research*, Vol. 31, May 1994, pp.111-118.

[13] R. Teodorescu and F. Blaabjerg, Flexible control of small wind turbines with grid failure detection operating in stand-alone and grid-connected mode. *IEEE Transactions on Power Electronics*, Vol. 19, No. 5, September 2004, pp.1323-1332.

[14] J. L. Domínguez-García, O. Gomis-Bellmunt, L. Trilla-Romero and A. Junyent-Ferré, Indirect vector control of a squirrel cage induction generator wind turbine. *Computers and Mathematics with Applications,* Vol. 64, 2012, pp. 102–114.

[15] M. H. Haque, Voltage regulation of a stand-alone induction generator using thyristor-switched capacitors. *IEEE International Conference on Sustainable Energy Technologies ICSET'08*, November 2008, Singapore, pp-34-39.

[16] G.K. Singh, Self-excited induction generator research – a survey. *Electric Power Systems Research*, Vol. 69, 2004, pp. 107-114.

[17] G. S. Kumar and A. Kishore, Generalized state-space modeling of three phase self-Excited induction generator for dynamic characteristics and analysis. *Journal of Electrical Engineering & Technology*, Vol. 1, No. 4, 2006, pp. 482-489.

[18] S. Moulahoum and N. Kabache, Behaviour analysis of self excited induction generator feeding linear and no linear loads. *Journal of Electrical Engineering & Technology*, Vol. 8, No. 6, 2013, pp. 1371-1379.

[19] D. Iannuzzi, D. Lauria and M. Pagano, Advanced statcom control for stand alone induction generator power sources. *International Symposium on Power Electronics Electrical Drives Automation and Motion SPEEDAM, IEEE*, 2008, pp. 60-65.

[20] K. H.Youssef, M. A. Wahba, H. A. Yousef and O. A. Sebakhy, A new method for voltage and frequency control of stand-alone self-excited induction generator using PWM converter with variable DC link voltage. *American Control Conference ACC'08*, June 2008, Washington, pp. 2486-2491.

[21] A. Karthikeyan, C. Nagamani, G. S. Ilango and A. Sreenivasulu, Hybrid, Open-loop excitation system for a wind turbine-driven stand-alone induction generator. *IET Renewable Power Generation*, Vol. 5, No. 2, 2011, pp. 184–193.

[22] A.Nesba, R. Ibtiouen, O. Touhami, Dynamic performances of self-excited induction generator feeding different static loads. *Serbian Journal of Electrical Engineering*, Vol. 3, No. 1, June 2006, pp.63-76.

[23] A. K. Tiwari, S.S. Murthy, B. Singh and L. Shridhar, Design-based performance evaluation of two-winding capacitor self-excited single-phase induction generator. *Electric Power Systems Research,* Vol. 67, 2003, pp. 89-97.